Multidomain Formulation of BEM Analysis Applied to Large-Scale Polycrystalline Materials

A. F. Galvis[1]**, R. Q. Rodriguez**[1] **P. Sollero**[1] **and E. L. Alburquerque**[2]

Abstract: Polycrystalline structures are present on metal alloys. Therefore, it is necessary to understand and model the mechanical behavior of this media. Usually, this is accomplished by the use of different numerical methods. However, the analysis of polycrystalline materials leads to other type of problems, such as high computational requirements generated in order to get an efficient solution. In this work, the 2D polycrystalline structure is generated using an average grain size through the Voronoi tessellation method and discretized through simulations with random material, crystalline orientation and orthotropic behavior [Sfantos and Aliabadi (2007a)]. BEM discretization requires multidomain analysis and large-scale degrees of freedom [Katsikadelis (2002);Kane (1994)]. This technique demands a different strategy in order to get a faster response. Numerical examples were carried out to demonstrate the feasibility of the application of the method to large-scale polycrystalline problems. Results were compared with the conventional BEM solution for several set of loads. The analysis of the structure is performed using the proposed anisotropic multidomain BEM formulation [Katsikadelis (2002);Kane (1994)].

Keywords: Multidomain Boundary Element Method, Polycrystalline Materials.

1   Introduction

The Boundary Element Method (BEM) is a powerful numerical method for the solution of different problems in engineering [Rodriguez, Sollero, and Alburquerque (2012)]. However, the BEM has some disadvantages when compared with other methods, mainly due to the fully populated matrices that are generated and the high computational load required during its process. [Sfantos and Aliabadi (2007a)] used the BEM for polycrystalline structure analysis, they investigated 2D crack propagation along grain boundaries through a linear cohesive law, and mixed mode

---

[1] UNICAMP, Campinas, SP, Brazil.
[2] UnB, Brasilia, DF, Brazil.

failure conditions. [Dong and Atluri (2013)] developed the symmetric-Galerkin boundary element method (SGBEM) with SGBEM Voronoi Cells (SVC) for direct two-dimentional micromechanical numerical modeling of heterogeneous composites where each SVC can include micro-inhomogeneities such inclusions, voids and cracks. [Benedetti and Aliabadi (2013)] applied techniques for homogenization of a three dimensional model of cubic polycrystalline material. [Dong and Atluri (2012)] used three-dimensional Trefftz Voronoi Cells with ellipsoidal voids /inclusions which are developed for micromechanical modeling of heterogeneous materials. [Sfantos and Aliabadi (2007b)] proposed a multi-scale BEM modellig for material and degradation fracture. Molecular dynamics simulation was carried out by [Nishimura and Miyazaki (2001)] to determinate the crack propagation in polycrystalline materials. [Dong and Atluri (2011)] used three different approaches to derive T-Trefftz Voronoi Cell Finite Elements for micromechanical analysis of heterogeneous materials. [Kokaly, Tran, Kobayashi, Dai, Patel, and White (2000)] used the implementation of another numerical method to generate a two-dimensional finite element (FE) model of assembly with idealized microstructure and uniform grain size of polycrystalline alumina. [Dawson, Boyce, and Rogge (2005)] employed multiscale approaches to modeling evolution of the material structure during deformation processes.

Large-scale polycrystalline material modeling requires the use of muldomain BEM that is widely explained by [Kane (1994);Katsikadelis (2002)], both suggested a different strategy to generate the array of hypermatrices. Recently, several numerical methods for solving these large systems of equations have been developed in order to reduce the time of execution. The Adaptive Cross Approximation (ACA) was used by [Grytsenko and Peratta (2008)] as a solver for three-dimension singular domain BEM application. An OUT-CORE solver for large, multi-zone boundary element matrices is presented by [Rigby and Aliabadi (1995)] and Block Equation Solver (BES) are developed by [Kane (1994);Crotty (1982)] that uses the Gaussian Elimination by blocks for linear elasticity BEM problems.

In this paper the implementation of multidomain formulation of BEM by [Kane (1994)] is performed over polycrystalline structure generated with anisotropic fundamental solution and the application of Blocked Equation Solver is proposed. Finally, conclusions are pointed out.

2   Polycrystalline Structure Modeling

The material modeling used in this work is the generation of a random artificial structure with the Voronoi tessellation method as in [Sfantos and Aliabadi (2007a)]; this approach defines the behavior of the structure with random orthotropic material and crystalline orientation. The simulation was performed as shown in Fig. 1.
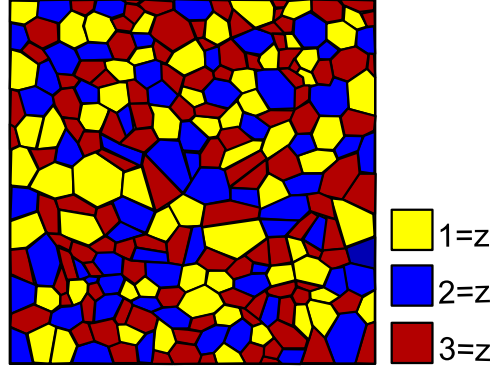
Figure 1: Artificial structure generated with randomly distributed material orientation for each grain

Due to the formulation used in this paper, the material orientation coordinated axes 123 coincides with the geometrical coordinate system xyz, that means $\theta = 0$. Different cases are taken into consideration when each axis coincides with the axis z of the geometry coordinated system; thus case $1 \equiv z$, case $2 \equiv z$ and case $3 \equiv z$. These cases are presented in three different colors in Fig. 1.

Grain material properties are modeled for plain strain and plain stress analysis with the following constitutive relations Eq. 1.

$$\sigma_{ij} = c_{ijkl}\varepsilon_{kl}, \qquad\qquad \varepsilon_{ij} = s_{ijkl}\sigma_{kl} \qquad\qquad (1)$$

where c_{ijkl} is the stiffness tensor and s_{ijkl} is the compliance tensor using the Voigt notation Eq. 2 that is defined by [Sfantos and Aliabadi (2007a);Rousselier, Barlat, and Yoon (2009)].

$$\mathbf{s} = [s_{ij}], (i, j = 1, 2, ..., 6) \qquad\qquad (2)$$

For the case of orthotropic material with three mutually perpendicular symmetry planes, the compliance tensor is reduce to 9 components, since $s_{14} = s_{15} = s_{16} = 0$, $s_{24} = s_{25} = s_{26} = 0$, $s_{34} = s_{35} = s_{36} = 0$ and $s_{45} = s_{46} = s_{56} = 0$.

In polycrystalline structure, three abovementioned cases are considered for modeling. The compliance tensor takes the following form:

$$s' = \begin{bmatrix} s'_{11} & s'_{12} & s'_{16} \\ & s'_{22} & s'_{26} \\ sym & & s'_{66} \end{bmatrix} \tag{3}$$

In Tab. 1 is shown the compliance tensor for the case of plane stress and in Tab. 2 the compliance tensor for the case of plane strain is presented.

Table 1: Compliance tensor components for two-dimensional plane stress case

s'_{ij}	$1 \equiv \mathbf{z}$	$2 \equiv \mathbf{z}$	$3 \equiv \mathbf{z}$
$\mathbf{s'_{11}}$	s_{22}	s_{11}	s_{11}
$\mathbf{s'_{22}}$	s_{33}	s_{33}	s_{22}
$\mathbf{s'_{12}}$	s_{23}	s_{13}	s_{12}
$\mathbf{s'_{66}}$	s_{44}	s_{55}	s_{66}

Table 2: Compliance tensor components for two-dimensional plane strain case

$1 \equiv \mathbf{z}$	$2 \equiv \mathbf{z}$	$3 \equiv \mathbf{z}$
$s'_{ij} = s_{kl} - \dfrac{s_{k1}s_{l1}}{s_{11}}$	$s'_{ij} = s_{kl} - \dfrac{s_{k2}s_{l2}}{s_{22}}$	$s'_{ij} = s_{kl} - \dfrac{s_{k3}s_{l3}}{s_{33}}$
$\left\{ \begin{matrix} i,j \\ k,l \end{matrix} \right\} = \left\{ \begin{matrix} 1,2,6 \\ 2,3,4 \end{matrix} \right\}$	$\left\{ \begin{matrix} i,j \\ k,l \end{matrix} \right\} = \left\{ \begin{matrix} 1,2,6 \\ 1,3,5 \end{matrix} \right\}$	$\left\{ \begin{matrix} i,j \\ k,l \end{matrix} \right\} = \left\{ \begin{matrix} 1,2,6 \\ 1,2,6 \end{matrix} \right\}$

3   Anisotropic Fundamental Solution

The displacement fundamental solution Eq. 4 and traction fundamental solution Eq. 5 for two-dimensional elastostatic problems are given by [Sollero and Aliabadi (1993)].

$$U_{ij}\left(z'_k, z_k\right) = 2\text{Re}\left[p_{j1}A_{i1}\ln\left(z_1 - z'_1\right) + p2A_{i1}\ln\left(z_2 - z'_2\right)\right] \tag{4}$$

$$T_{ij}\left(z'_k, z_k\right) = 2\text{Re}\left[\frac{1}{\left(z_1 - z'_1\right)}q_{j1}\left(\mu_1 n_1 - n_2\right)A_{i1} - \frac{1}{\left(z_2 - z'_2\right)}q_{j2}\left(\mu_2 n_1 - n_2\right)A_{i2}\right] \tag{5}$$

where z'_k, is the source point Eq. 6

$$z'_k = x'_1 + \mu_k x'_2 \tag{6}$$

and z_k, is the field point Eq. 7

$$z_k = x_1 + \mu_k x_2 \tag{7}$$

μ_k are the complex roots of the characteristic polynomial Eq. 8 and always are pure imaginary or conjugate pair.

$$s'_{11}\mu^4 - 2s'_{16}\mu^3 + (2s'_{12} + s'_{16})\mu^2 - 2s'_{26}\mu + s'_{22} = 0 \tag{8}$$

the terms p_{ij} and q_{ij} are given by

$$p_{ik} = \begin{bmatrix} s'_{11}\mu_k^2 + s'_{12} - s'_{16}\mu_k \\ s'_{11}\mu_k + s'_{22}/\mu_k - s'_{16} \end{bmatrix} \tag{9}$$

and

$$q_{ik} = \begin{bmatrix} \mu_1 & \mu_2 \\ -1 & -1 \end{bmatrix} \tag{10}$$

The complex coefficients A_{ij} are obtained with the solution of the following complex linear system of equations

$$\begin{bmatrix} 1 & -1 & 1 & -1 \\ \mu_1 & \bar{\mu}_1 & \mu_2 & \bar{\mu}_2 \\ p_{11} & -\bar{p}_{11} & p_{12} & -\bar{p}_{12} \\ p_{21} & -\bar{p}_{21} & p_{22} & -\bar{p}_{22} \end{bmatrix} \begin{Bmatrix} A_{j1} \\ \bar{A}_{j1} \\ A_{j2} \\ \bar{A}_{j2} \end{Bmatrix} = \begin{Bmatrix} \delta_{j2}/2\pi i \\ -\delta_{j1}/2\pi i \\ 0 \\ 0 \end{Bmatrix} \tag{11}$$

where δ_{ij} is the Kronecker delta.

4 Multidomain Boundary Element Method

The application of BEM over polycrystalline structure problems demands the use of multidomain formulation [Kane (1994);Katsikadelis (2002)]. As mentioned before, the material structure has different properties of elasticity and orientation cases per grain. BEM is applied for each grain using the *Somigliana's identity* [Kane (1994)] Eq. 12 and constant boundary elements.

$$\int_\Gamma t_i U_{ij}^* d\Gamma = \int_\Gamma T_{ij}^* u_i d\Gamma + c_{ik} u_i (\mathbf{d}) \tag{12}$$

where U_{ij}^* and T_{ij}^* are the displacement and traction fundamental solution respectively. The Eq. 12 is applied over the boundary Γ with the source point located in **d**.

In multidomain formulation, there are two kind of grains, when the grain is in the boundary and when it is an internal grain [Sfantos and Aliabadi (2007a)]. However, only a portion of boundary grains have defined boundary conditions. Therefore, the number of unknowns belonging to internal grains and part of the boundary grains exceeds the number of equations, [Kane (1994);Katsikadelis (2002)]. In order to get a feasible system for the solution, traction equilibrium and displacement compatibility Eq. 13 are applied at the interfaces [Kane (1994)].

$$t_{ij}^i = -t_{ji}^j \qquad\qquad u_{ij}^i = u_{ji}^j \tag{13}$$

In order to illustrate the multidomain formulation, Fig. 2 shows a three-zone BEA model and then the description of the formulation is performed.
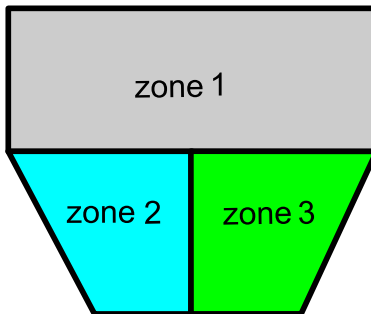

Figure 2: Three-Multidomain model

Initiating with the boundary integral equation applied in the zone 1

$$[\mathbf{H}]^1\{\mathbf{u}\}^1 = [\mathbf{G}]^1\{\mathbf{t}\}^1 \tag{14}$$

Dividing both matrices **H** and **G** by their respective counterparts matrices corresponding to the boundary and the interface

$$\begin{bmatrix} [\mathbf{H}]^1_1 & [\mathbf{H}]^1_{12} & [\mathbf{H}]^1_{13} \end{bmatrix} \left\{ \begin{array}{c} \{\mathbf{u}\}^1_1 \\ \{\mathbf{u}\}^1_{12} \\ \{\mathbf{u}\}^1_{13} \end{array} \right\} = \begin{bmatrix} [\mathbf{G}]^1_1 & [\mathbf{G}]^1_{12} & [\mathbf{G}]^1_{13} \end{bmatrix} \left\{ \begin{array}{c} \{\mathbf{t}\}^1_1 \\ \{\mathbf{t}\}^1_{12} \\ \{\mathbf{t}\}^1_{13} \end{array} \right\} \tag{15}$$

applying equation Eq. 13 and boundary conditions of external part of the zone 1

$$\begin{bmatrix} [\mathbf{A}]^1_1 & [\mathbf{H}]^1_{12} & [\mathbf{H}]^1_{13} \end{bmatrix} \left\{ \begin{array}{c} \{\mathbf{x}\}^1_1 \\ \{\mathbf{u}\}^1_{12} \\ \{\mathbf{u}\}^1_{13} \end{array} \right\} = \{\mathbf{b}\}^1_1 + \begin{bmatrix} -[\mathbf{G}]^1_{12} & [\mathbf{G}]^1_{13} \end{bmatrix} \left\{ \begin{array}{c} \{\mathbf{t}\}^1_{12} \\ \{\mathbf{t}\}^1_{13} \end{array} \right\}$$

$$\tag{16}$$

In Eq. 15, matrices $[\mathbf{H}]^1_1$ and $[\mathbf{G}]^1_1$ are only for the zone 1 before the application of boundary conditions, matrices $[\mathbf{H}]^1_{12}$ and $[\mathbf{H}]^1_{13}$ are the terms of the interface between the zones 1 and zone 2 and between zone 1 and zone 3, respectively, vectors $\{\mathbf{x}\}^1_1$ and $\{\mathbf{b}\}^1_1$, Eq. 16 contains all the unknown and known boundary quantities of zone 1, respectively, the matrix $[\mathbf{A}]^1_1$ resulting after the application of the known boundary conditions.

Following the same scheme to generate the equation for the zone 2

$$\begin{bmatrix} [\mathbf{H}]^2_2 & [\mathbf{H}]^2_{12} & [\mathbf{H}]^2_{23} \end{bmatrix} \left\{ \begin{array}{c} \{\mathbf{u}\}^2_2 \\ \{\mathbf{u}\}^2_{12} \\ \{\mathbf{u}\}^2_{23} \end{array} \right\} = \begin{bmatrix} [\mathbf{G}]^2_2 & [\mathbf{G}]^2_{12} & [\mathbf{G}]^2_{23} \end{bmatrix} \left\{ \begin{array}{c} \{\mathbf{t}\}^2_2 \\ \{\mathbf{t}\}^2_{12} \\ \{\mathbf{t}\}^2_{23} \end{array} \right\} \tag{17}$$

applying equation Eq. 13 and boundary conditions of external part of the zone 2

$$\begin{bmatrix} [\mathbf{A}]^2_2 & [\mathbf{H}]^2_{12} & [\mathbf{H}]^2_{23} \end{bmatrix} \left\{ \begin{array}{c} \{\mathbf{x}\}^2_2 \\ \{\mathbf{u}\}^1_{12} \\ \{\mathbf{u}\}^2_{23} \end{array} \right\} = \{\mathbf{b}\}^2_2 + \begin{bmatrix} -[\mathbf{G}]^2_{12} & [\mathbf{G}]^2_{23} \end{bmatrix} \left\{ \begin{array}{c} \{\mathbf{t}\}^1_{12} \\ \{\mathbf{t}\}^2_{23} \end{array} \right\}$$

$$\tag{18}$$

similarly for the zone 3

$$
\left[\ [\mathbf{A}]_3^3\ \ [\mathbf{H}]_{13}^3\ \ [\mathbf{H}]_{23}^3\ \right]
\left\{
\begin{array}{c}
\{\mathbf{x}\}_3^3 \\
\{\mathbf{u}\}_{13}^1 \\
\{\mathbf{u}\}_{23}^2
\end{array}
\right\}
= \{\mathbf{b}\}_3^3 +
\left[\ -[\mathbf{G}]_{13}^3\ \ -[\mathbf{G}]_{23}^3\ \right]
\left\{
\begin{array}{c}
\{\mathbf{t}\}_{13}^1 \\
\{\mathbf{t}\}_{23}^2
\end{array}
\right\}
\tag{19}
$$

with Eq. 16, Eq. 18 and Eq. 19 is possible to obtain the general matrix system array for the problem with the form $[\mathbf{A}]\{\mathbf{x}\} = \{\mathbf{b}\}$, combining the above equations:

$$
[\mathbf{A}] =
\left[
\begin{array}{ccccccccc}
[\mathbf{A}]_1^1 & [\mathbf{H}]_{12}^1 & [\mathbf{H}]_{13}^1 & -[\mathbf{G}]_{12}^1 & [0] & [0] & -[\mathbf{G}]_{13}^1 & [0] & [0] \\
[0] & [\mathbf{H}]_{12}^2 & [0] & [\mathbf{G}]_{12}^2 & [\mathbf{A}]_2^2 & [\mathbf{H}]_{23}^2 & [0] & -[\mathbf{G}]_{23}^2 & [0] \\
[0] & [0] & [\mathbf{H}]_{13}^3 & [0] & [0] & [\mathbf{H}]_{23}^3 & [\mathbf{G}]_{13}^3 & [\mathbf{G}]_{23}^3 & [\mathbf{A}]_3^3
\end{array}
\right]
\tag{20}
$$

The $\{\mathbf{x}\}$ Eq. 21 is the vector that contains the unknown values of the external boundary and interfaces and $\{\mathbf{b}\}$ Eq. 22 is the known vector.

$$
\{\mathbf{x}\} = \left\{\ \{\mathbf{x}\}_1^1\ \ \{\mathbf{u}\}_{12}^1\ \ \{\mathbf{u}\}_{13}^1\ \ \ \{\mathbf{t}\}_{12}^1\ \ \{\mathbf{x}\}_2^2\ \ \{\mathbf{u}\}_{23}^2\ \ \ \{\mathbf{t}\}_{13}^1\ \ \{\mathbf{t}\}_{23}^2\ \ \{\mathbf{x}\}_3^3\ \ \right\}^{\mathsf{T}}
\tag{21}
$$

$$
\{\mathbf{b}\} = \left\{\ \{\mathbf{b}\}_1^1\ \ \{\mathbf{b}\}_2^2\ \ \{\mathbf{b}\}_3^3\ \right\}^{\mathsf{T}}
\tag{22}
$$

5   Blocked Equation Solver

The Multidomain BEM formulation generates a general system of equations where matrix $[\mathbf{A}]$ is a hypermatrix like Eq. 20, and its entries are smaller matrices [Kane (1994)]. These kind of matrices are sparse. For the polycrystalline structures that is large-scale problem, a big percentage of the matrix will be zero due to the majority of subdomains are internal grains with unknown boundary conditions. In order to solve the equation system, the use of conventional methods can be inefficient. Thus the Blocked Equation Solver [Kane (1994)] is proposed as another way to obtain the solution. The strategy treats the hypermatrix as a division per blocks and has three different phases the *BlockFactorization*, *Black − forward Reduction* and *Block − BackSubstitution*.

The division of the matrix in blocks depends on the problem; and appropriated hypermatrix is required in order to apply this method. Therefore is strongly necessary to have nonzero blocks in the main diagonal. This is possible using the presented array matrix Eq. 20 proposed by [Kane (1994);Crotty (1982)]. However, its implementation can be more complex than the suggested by [Katsikadelis (2002)], where part of the diagonal blocks are zero leading the method fail. the proposed method in this work is determined with the size of the overall matrix Eq. 20 and the size of the square matrix $[\mathbf{H}]$ for each subdomain located it in the main diagonal of the of the overall matrix. Completed system of equations divided per blocks is shown in Eq. 23 [Kane (1994)].

$$
\begin{bmatrix}
[\mathbf{A}_{11}] & [\mathbf{A}_{12}] & [\mathbf{A}_{13}] \\
[\mathbf{A}_{21}] & [\mathbf{A}_{22}] & [\mathbf{A}_{23}] \\
[\mathbf{A}_{31}] & [\mathbf{A}_{32}] & [\mathbf{A}_{33}]
\end{bmatrix}
\left\{
\begin{array}{c}
\{\mathbf{x}_1\} \\
\{\mathbf{x}_2\} \\
\{\mathbf{x}_3\}
\end{array}
\right\}
=
\left\{
\begin{array}{c}
\{\mathbf{b}_1\} \\
\{\mathbf{b}_2\} \\
\{\mathbf{b}_3\}
\end{array}
\right\}
\tag{23}
$$

The method is based on the $[\mathbf{L}][\mathbf{U}]$ factorization on the main diagonal and used matrix multiply and subtract operation between different matrices and vectors from the overall system. The iterative process is shown in [Kane (1994)], and is used to develop a general algorithm for random polycrystalline structure in which the matrix has a random block division in the diagonal. An advantage of this method is that the only extra memory needed for the alterations of the blocks from the overall matrix is when the matrix $[\mathbf{D}]$ is calculated, for more details see [Kane (1994)].

6 Numerical Results

Simulation performed in this work is for 2090-T3 aluminum lithium alloy [Rousselier, Barlat, and Yoon (2009)]. The components of the stiffness tensor are presented in Tab. 3 for plane strain analysis and the material is generated with a virtual polycrystalline structure as abovementioned with random orientation and orthotropic behavior is shown in Fig. 1.

Table 3: Stiffness tensor of 2090-T3 aluminum lithium alloy (GPa)

C_{11}	C_{12}	C_{13}	C_{21}	C_{22}	C_{32}	C_{33}	C_{44}	C_{55}	C_{66}
981.19	7.06	3.15	40.76	592.23	422.67	1018.80	1.28	368.22	834.81

The boundary conditions of the analyzed numerical example are shown in Fig. 3

In Fig. 4 is shown the pre-processing, in this paper constant boundary elements and anisotropic fundamental solution were used, six different polycrystalline structures were generated for 10, 20, 50, 100 and 300 grains and load of 10 N
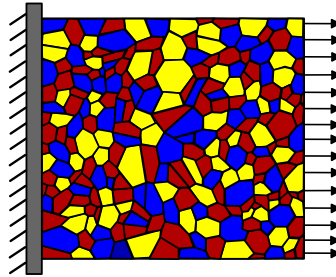
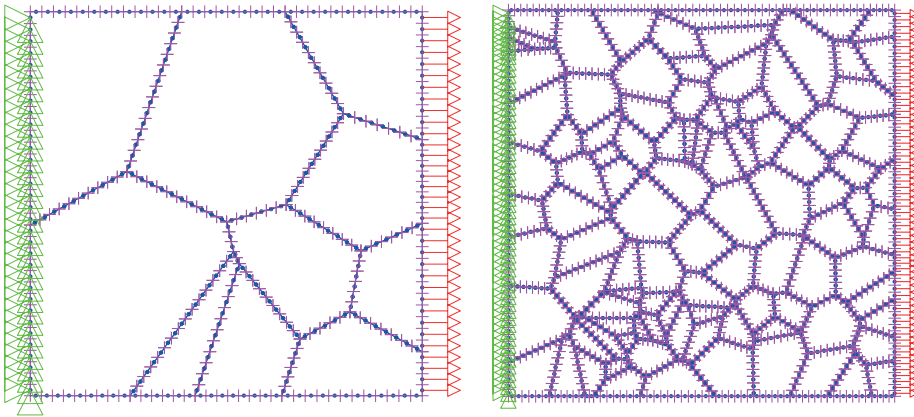Figure 3: Boundary Conditions for the polycrystalline structure

Figure 4: Pre-processing examples for 10 grains (430 elements) and 100 grains (2515 elements)

Time results of the six simulations performed are given in Tab. 4.

Table 4: Time require for different methods to solve the system

Grains	Unkowns	Time (s)			
		Inverse	LU Fractorization	Gauss	BES
10	860	0.0486	0.0243	0.0248	0.0411
20	1352	0.1692	0.07165	0.07122	0.07182
50	2884	1.495	0.4785	0.4814	0.4161
100	5030	7.2055	2.0185	2.0477	1.789
150	9828	51.028	13.923	13.046	7.6177
300	15970	205.554	52.032	52.283	39.072

Comparisons between the Block Equation Solver and different Matlab Solvers like inverse, LU factorization and Gauss are given in Fig. 5, where is possible to observe the differences between the methods.
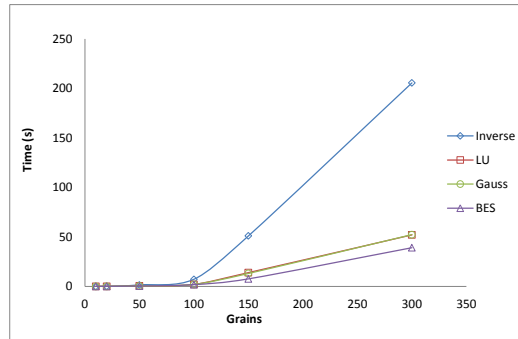

Figure 5: Time comparison between the Block Equation Solver and Matlab Solver

7 Conclusions

In this work, a Block Equation Solver (BES), based on [Kane (1994)], was adapted to multidomain Polycrystalline large-scale problems. This methodology showed to be efficient when compared with the conventional Matlab solver in Fig. 5. This is mainly because a multidomain problem can be easily adapted to a block solver. However, the collocation matrix structure could be assembled by several approaches, such as [Katsikadelis (2002);Kane (1994)], and this fact affects directly the proposed strategy. The BES works better where more than 40 grains are analyzed.

References

Benedetti, I.; Aliabadi, M. (2013): A three-dimensional grain boundary formulation for microstructural modeling of polycrystalline materials. *Computational Materials Science*, vol. 67, pp. 249–260.

Crotty, J. (1982): A block equation solver for large unsymmetric matrices arising in the boundary integral equation. *International Journal For Numerical Methods In Engineering*, vol. 18, pp. 997–1017.

Dawson, P.; Boyce, D.; Rogge, R. (2005):   Issues in modeling heterogeneous deformations in polycrystalline metals using multiscale approaches. *CMES: Computer Modeling in Engineering & Science*, vol. 10, no. 2, pp. 123–141.

Dong, L.; Atluri, S. (2011):   Development of T-Trefftz four-node quadrilateral and voronoi cell finite elements for macro- & micromechanical modeling of solids. *CMES: Computer Modeling in Engineering & Science*, vol. 81, no. 1, pp. 69–118.

Dong, L.; Atluri, S. (2012):   Development of 3D trefftz voronoi cells with ellipsoidal voids &/or elastic/rigid inclusions for micromechanical modeling of heterogeneous materials. *CMC: Computers, Materials & Continua*, vol. 30, no. 1, pp. 39–81.

Dong, L.; Atluri, S. (2013):   SGBEM voronoi cells (SVCs), with embedded arbitrary-shaped inclusions, voids, and/or cracks, for micromechanical modeling of heterogeneous materials. *CMC: Computers, Materials & Continua*, vol. 33, no. 2, pp. 111–154.

Grytsenko, T.; Peratta, A. (2008):   Adaptive cross approxiamtion based solver for boundary element method with single domain in 3D. In *Boundary Element Method and Other Mesh Reduction Methods XXX*.

Kane, J. (1994):   *Boundary Element Analysis In Engineering Continuum Mechanics*. Prentice-Hall.

Katsikadelis, J. (2002):   *Boundary Elements: Theory and Applications*. Elsevier Science.

Kokaly, M.; Tran, D.; Kobayashi, A.; Dai, X.; Patel, K.; White, K. (2000): Modelling of grain pull-out forces in polycrystalline alumina. *Materials Science and Engineering*, vol. A285, pp. 151–157.

Nishimura, K.; Miyazaki, N. (2001):   Molecular dynmics simulation of crack propagation in polycrystalline materials. *CMES: Computer Modeling in Engineering & Science*, vol. 2, no. 5, pp. 143–154.

Rigby, R.; Aliabadi, M. (1995):   OUT-OF-CORE solver for large, multizone boundary element matrices. *International Journal For Numerical Methods In Engineering*, vol. 38, pp. 1507–1533.

Rodriguez, R.; Sollero, P.; Alburquerque, E. (2012):   Analysis of anisotropic symmetric plates by adaptive cross approximation. In *International Conference on Boundary Element and Meshless Techniques XIII*.

Rousselier, G.; Barlat, F.; Yoon, J. (2009):   A novel approach for anisotropic hardening modeling. part 1: Theory and its application to finite element analysis of deep drawing. *International Journal of Plasticity*, vol. 25, pp. 2383–2409.

Sfantos, G. K.; Aliabadi, M. H. (2007): A boundary cohesive grain element formulation for modelling intergranular microfracture in polycrystalline brittle materials. *International Journal For Numerical Methods In Engineering*, vol. 69, pp. 1590–1626.

Sfantos, G. K.; Aliabadi, M. H. (2007): Multi-scale boundary element modelling of material degradation and fracture. *Computer Methods in Applied Mechanics and Engineering*, vol. 196, pp. 1310–1329.

Sollero, P.; Aliabadi, M. (1993): Fracture mechanics analysis of anisotropic plates by the boundary element method. *International Journal of Fracture*, vol. 64, pp. 269–284.